Modelling the Dynamic Response of
Monopile Foundations for Wind Turbines

By
Jamie Munro (CHU)

Fourth-year Undergraduate Project
Group D, 2012/2013

Supervisor: Dr SPG Madabhusi

"I hereby declare that, except where specifically indicated, the work submitted herein is my own original work."

Signed: _________________________ Date: _____________

Technical Abstract

Modelling the dynamic response of monopile foundations for wind turbines

In recent years there has been a drive for renewable energy generation. Wind farms, whether onshore or offshore, are sources of renewable energy and the wind energy industry has shown rapidly increasing growth over the last twelve years. For this increasing trend to continue the cost of constructing and maintaining the wind farm must better balance the revenue generated from the energy it produces. Improvements must be made if wind energy is to remain a viable option compared to other energy sources.

The cost of the support structure for a wind turbine is a significant proportion of the construction cost. A typical foundation for an offshore wind turbine is a driven monopile. Monopiles are typically used in shallow water conditions, conditions that are typical around much of the United Kingdom. To make these foundations more economic the structures behaviour needs to be better understood. Current design methodologies are based on smaller diameter piles for use in the oil and gas industries. They are being used outside of their verified range when applied to large diameter monopiles. They also do not account accurately for the dynamic nature of the loading applied to wind turbines.

Numerical modelling of the situation relies on having accurate constitutive models for the soil that take into account the non-linear stress-strain behaviour. Analytical models usually over-simplify the soil-structure interaction effects. Full-scale testing is expensive and not very controllable. This aim of this project was to use small-scale models of the turbine-foundation-soil system in laboratory conditions at 1-g acceleration levels to gain a qualitative insight into the system's dynamic response.

Tests were conducted on a small aluminium model monopile driven into a large tub of dry sand. The pile itself and the surrounding sand were instrumented with micro-electro-mechanical accelerometers to record the models response to the loading.

Impulse loading was applied to the model to identify the natural frequency of the system. Impulse loading also allowed the assessment of shear wave velocity through the soil. One-directional harmonic loading over a range of driving frequencies was applied to the model

using a piezoelectric actuator. The harmonic loading allowed observation of how the response of the monopile and surrounding soil varied with forcing frequency.

Analysis showed that there were significant increases in natural frequency and shear wave velocity as the density of the sand was increased. The denser sand was clearly increasing the stiffness of the system and this shows that pile-soil interaction shouldn't be neglected in dynamic design. Shear wave velocities were significantly higher than predicted by empirical formulations; the variation with soil density also seemed to be more significant. However it should be noted that the empirical formulations used are based upon much larger soil stresses than could be generated at 1-g acceleration levels in the laboratory. Analysis also showed that as expected damping was much higher when the pile was embedded in the sand. Looser sand provided higher levels of damping than dense sand.

Further analysis of impulse and harmonic responses in both the time and frequency domain using wavelet analysis showed that higher frequency components of the response developed in the soil further away from the pile. Despite the overall reduced magnitude the development of higher frequency components could become a concern if there is sensitive equipment nearby or if the vibrations develop into a range that is an annoyance to nearby residents.

This project has investigated how changing soil density influences the pile-soil interaction, future work could benefit from investigating how changing pile properties influences the pile-soil interaction. It is suggested that the impact of changing the flexibility of the pile is investigated through similar testing. A model monopile of the same dimensions but made from PVC would be a more flexible alternative.

Qualitative insight into the dynamic response of the system has been gained through this project. It would be beneficial to take some of the techniques developed throughout the course of this project and use them in geotechnical centrifuge models or full-scale testing which would then allow some quantitative results to be generated that may be applied to real design.

Acknowledgements

I would like to thank my supervisor, Dr Madabhusi, for his help and guidance with this project over the last year. I would also like to thank the technicians and graduate students at the Schofield Centre whose help was instrumental in the completion of this project. Finally I would like to specifically thank Charlie Heron for his help with experimental setup and guidance in using MATLAB for data analysis.

Contents

Nomenclature

G	Soil Shear Modulus	(N/m^2)
E_p	Young's Modulus of Pile	(N/m^2)
D	Pile Diameter	(m)
I_{xx}	Pile Second Moment of Area	(m^4)
I_d	Relative Density of Sand	(-)
M	Mass concentrated at Turbine Top	(kg)
M_{eq}	Equivalent Mass of SDOF System	(kg)
K_{eq}	Equivalent Stiffness of SDOF System	(N/m)
K_L	Lateral Stiffness	(N/m)
K_R	Rotational Stiffness	(Nm/rad)
K_o	Coefficient of Earth Pressure	(-)
G_s	Specific Gravity	(-)
L	Total Length of Pile	(m)
L_e	Embedded Length of Pile	(m)
e	Voids Ratio	(-)
f_n	Natural Frequency of Pile	(Hz)
m	Mass per unit Length of Pile	(kg/m)
t	Pile Wall Thickness	(m)
p	Lateral Soil Resistance	(N/m)
p'	Mean Effective Stress	(N/m^2)
v_s	Shear Wave Velocity	(m/s)
y	Lateral Displacement	(m)
z	Depth below soil surface	(m)
ν	Poisson's Ratio	(-)
ρ	Density of Material	(kg/m^3)
γ_{sand}	Unit Weight of Material	(N/m^3)
σ'	Soil Effective Stress	(N/m^2)
γ	Shear Strain	(-)

1.0 Introduction

1.1 The Demand for Wind Energy

Climate change and the depletion of natural resources are important international issues in today's world. Together they have led to a drive for national energy security and the advancement of renewable energy technology. Key targets for the United Kingdom include:

- 15% of energy consumed will be derived from renewable sources by 2020 (European Commission, 2008a).
- 80% less carbon emissions in 2050 than in 1990 (UK Government, 2008).

Energy consumed includes petrol used in transport infrastructure; it is not likely that this will decrease in the near future. It is predicted that in order to meet these targets 30-35% of generated electricity in the UK will have to be from renewable sources (BERR, 2008). In 2011 only 9.4% of generated electricity, and only 3.8% of consumed energy, came from renewable sources (Department of Energy & Climate Change, 2012). Clearly there is a still a long way to go before the imposed targets are met.

Both onshore and offshore wind farms present opportunities to generate renewable energy. Being surrounded by relatively shallow water means that the UK is well positioned to benefit from energy production by offshore wind farms. Indeed recent trends show both the onshore and offshore wind farm industries are expanding rapidly. Both in terms of already constructed installations and those that have been granted consent to continue; this is illustrated in figure 1.1.

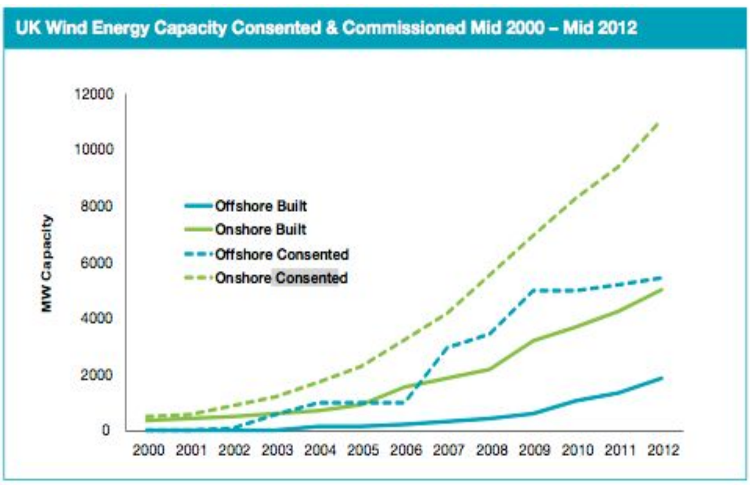

Figure1.1: Graph showing the increasing capacity of wind farms in the last twelve years (RenewableUK, 2012).

1.2 Offshore and Onshore Wind Farms

As figure 1.1 shows the UK has both onshore and offshore wind farm installations; figure 1.2 shows an example of both. There are advantages and disadvantages to both schemes. Generally offshore farms are considered to be more out of the way and subject to a more consistent wind that can lead to better power generation. There is also large room for expansion in the shallow waters around the UK. However there are increased costs due to more complicated foundations and the turbines must survive in much harsher working conditions.

Figure 1.2: (a) Thanet offshore wind farm (Photo: VATTENFALL) (b) Ardrossan onshore wind farm (Photo: Vincent van Zeijst).

On the other hand onshore installations generally have lower construction and maintenance costs. Although there is likely to be much more public objection due to concerns about the turbines ruining the natural beauty of the nearby land. There are also concerns about vibrations being transmitted through the ground as the turbine installations expand into areas closer to residents, as well as concerns about noise generated by the turbines.

The decision on where a wind farm is constructed is usually based on whether it is economically viable. This means that to actually get constructed a wind farm must have the potential to make more money in electricity generation than it costs to construct and maintain the installation. The two fundamental ways to address this profit-cost balance are to either increase the amount of electricity that a certain size of turbine can produce or to reduce the wind farm construction costs.

1.3 Offshore Monopile Foundations

A significant proportion of the offshore installation costs are associated with the foundation and support structure. These costs can typically be 1-4 million Euros, which is about 25-30% of the overall installation cost (LeBlanc, 2009). More efficient foundation designs will make wind farms economically more viable. For designs to be made more efficient the behaviour of the foundations needs to be better understood.

Wind turbines are tall structures that by their nature are often located in areas of high wind loading and in the offshore case will also experience lateral wave loading. As well as having sufficient vertical capacity the chosen foundation system must be capable of resisting the horizontal load and associated moment load that often dominate the design (Byrne & Houlsby, 2003). There are multiple foundations systems viable for offshore use, including: gravity base, multi-pile, monopile and suction caisson arrangements, shown schematically in figure 1.3. This project is concerned primarily with monopile foundations, which are a typical foundation system for wind turbines in shallow water, like the conditions found around the UK.

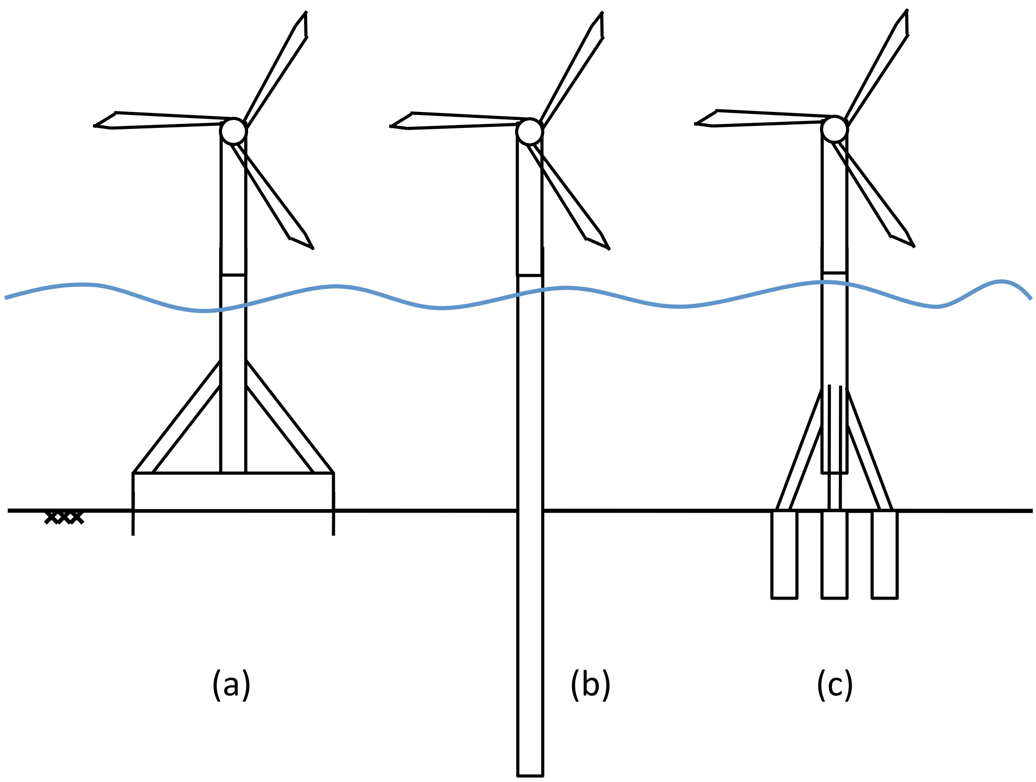

Figure 1.3: Schematic of different offshore foundation types (a) Skirted gravity base (b) Monopile (c) Multi-pile suction caisson arrangement.

Monopile foundations for offshore use are typically 4-6 m diameter hollow steel tubes with a wall thickness of 5-10 cm. These are then embedded into the ocean floor to depths typically 20-40m (LeBlanc, 2009). Piles may be either hammer driven directly into the seabed or may be inserted and grouted into a pre-bored shaft. Figure 1.4 shows the first monopile that was installed at the Anholt offshore wind farm in January 2012. Most simply monopiles are extensions of the turbine shaft; vertical capacity is achieved from shaft friction and lateral capacity by mobilising lateral soil resistance. The large diameters and wall thicknesses give a larger plastic moment capacity than the more conventional, smaller diameter piles. This allows the monopile to resist the large imposed moment loadings.

Figure 1.4: A 5m diameter, 45m long monopile ready for installation at the Anholt wind farm (Photo: DONG Energy, 2012).

Also the dynamic nature of the loading needs to be considered. As tall slender structures with a mass concentrated at the top they are dynamically sensitive, particularly as they are subject to a range of forcing frequencies. The main sources of dynamic load on a wind turbine (Adhikari & Bhattacharya, 2012) are:

- Dynamic loading caused by wind gusting (typically at frequencies around 0.02 Hz).
- Loading due to the action of waves against the turbine tower (typically at frequencies around 0.1 Hz).
- Inevitable out-of balance masses in the rotor assembly will lead to loading at the rotor frequency of the turbine – known as the 1P frequency (typically 0.3 Hz).

- There is also an effect where as the blades of the turbine pass in front of the tower they deflect the wind, causing another dynamic load. The frequency of this loading depends on the blade arrangement of the turbine. For a three-bladed turbine the loading will occur at three times the rotor frequency – therefore known as the 3P frequency.

These dynamic loads are shown in figure 1.5. It should also be noted that most modern wind turbines are fitted with variable speed rotor system so the 1P and 3P frequencies for a given turbine will actually be a frequency range, typically 0.17 to 0.33 Hz for the 1P frequency (Liingaard, 2006).

To avoid damage to the turbine the aim is often to design the turbine structure such that its natural frequencies are well separated from the forcing frequencies. Typically such that the fundamental frequency lies between the 1P and 3P frequencies, such a system is often described as being a Soft-Stiff system (Adhikari & Bhattacharya, 2012). The main problem in design is accounting for the soil-structure interaction. It is not accurate enough to simply model the turbine as a cantilever fixed at the mudline. As the natural frequency must lie in such a small range more sophisticated models are required.

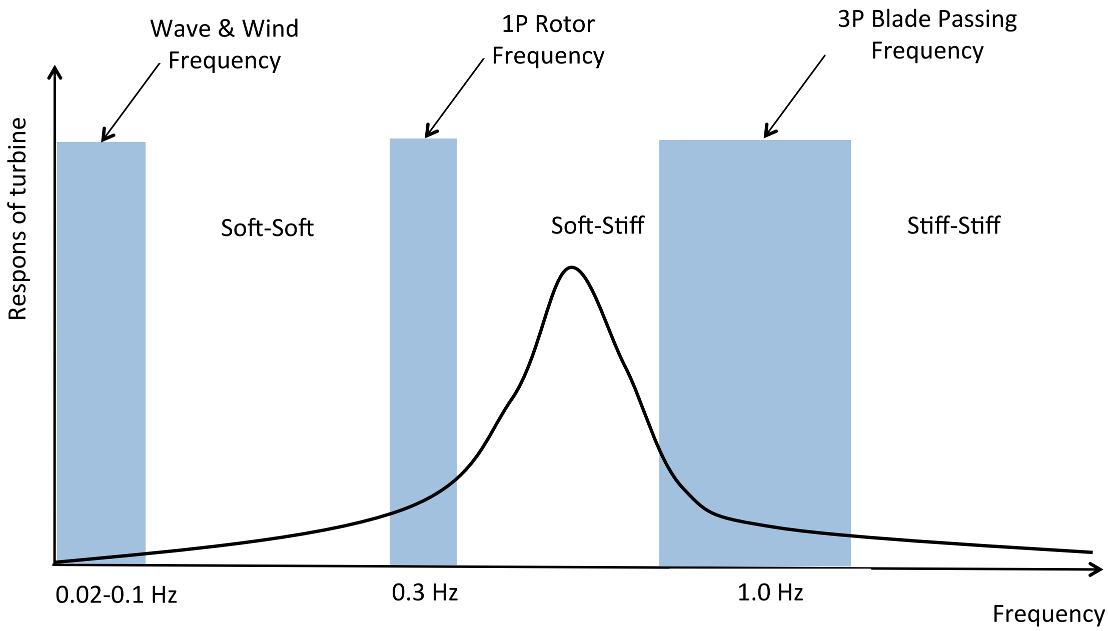

Figure 1.5: Typical main forcing frequencies on a wind turbine structure ((LeBlanc, Houlsby, & Byrne, 2010) & (Bhattacharya, Muir Wood, & Lombardi, 2011)).

1.4 Ground Borne Vibrations

As discussed wind turbines are dynamic structures and they will inevitably cause vibrations. It is important to design for the affects of this dynamic behaviour on the structure itself. However another issue is the transmission of these vibrations through the foundation and surrounding soil. This is particularly of concern for onshore wind farms. Concerns are primarily about residents feeling vibrations from the turbines and potential damage to nearby vibration-sensitive equipment.

Transmission of the vibrations will depend on the properties of the input itself, the frequency and magnitude. The transmission will also depend on the properties of the soil, its stiffness and how it dampens the vibrations. It is important to understand how far away from the turbine the vibrations travel before they are dampened to negligible magnitudes.

1.5 Project Objectives

In order to design better and more efficient structures in light of the issues discussed above it is desirable to know what variables have an influence and how they affect the mechanisms behind the problems. Physical modelling of the turbine-foundation-soil system in a laboratory setting helps to do this in a controlled manner. By scaling the foundations down into small models that can be constructed in a 850mm diameter tub the tests are quicker, cheaper, easier to observe and more controllable than at full scale. This project aims to use scaled physical models to:

- Investigate the natural frequency and damping characteristics of the monopile foundation and soil system.
- Investigate the ground borne vibrations caused by excitation of the foundation and how the stress waves decay around the monopile.

2.0 Literature Review

2.1 Current Pile Design

Currently adopted design methodologies for offshore wind farms such as the standard "Design of Offshore Wind Turbine Structures" (DNV, 2004) are based on guidelines in the standards DNV (1977) and API (1993) which are in turn based on p-y curves for piles in sand. These p-y curves show the relationship between the soil resistance mobilised 'p' as the pile displaces laterally by a distance 'y'. These were originally introduced by Reese & Matlock (1956). These relationships are based on empirical curves generally derived from full scale testing of piles (Reese & Impe, 2001). The p-y relationship can be used to solve the differential equations for beam bending used in designing the pile.

However the test piles and p-y curves were developed primarily for offshore use in the oil and gas industry. Both the size and flexibility of the piles and the nature of the loading differ between piles used in the oil-gas industry and the monopiles used to support wind turbines. LeBlanc, Houlsby, & Byrne (2010) argue that the p-y curves in their current form should not be used in the design of wind turbine support structures. The curves were derived for slender piles and in extrapolating up to the large diameter monopiles the p-y curves are being used outside of their verified range. The rigidity of the pile compared to the soil will have an impact on the systems behaviour (Briaud, Smith, & Meyer, 1984). A rigid pile, like a monopile, will tend to rotate about some point below the surface without much bending of the actual pile. This is unlike the failure mechanism that the p-y curve method is based on which assumes failure will occur when plastic hinges form in the pile. This is not typically the case for the failure of large monopiles (Lombardi, Bhatacharya, & Muir Wood, 2013). As the p-y curve method gives no way to account for the pile bending stiffness it does not properly account for the foundation-soil interaction effects (Brødæk, Møller, Sørensen, & Augustesen, 2009).

Another issue is that the allowance in the accepted design guidance for dealing with the cyclic nature of the loading is not entirely appropriate. The guidance is concerned more about the ultimate lateral capacity and ignores how accumulated displacements and rotations can alter the local soil stiffness (LeBlanc et al, 2010). The number of load cycles in a wind turbines design life could easily exceed 10^8 cycles and the p-y curves that have been derived for cyclic loading are based upon tests where only 200 cycles were applied (Achmus, Kuo, & Abdel-Rahman, 2009). For wind turbine support structures the displacements and rotations are likely to be more of a concern than the ultimate capacity of the monopile, wind turbines can typically not tolerate more than 0.5 degrees of tilt (Lombardi, Bhatacharya, & Muir Wood, 2013).

Accumulated displacements can be large in one direction due to the consistent nature of prevailing winds in the regions where wind farms are located. Repetitive lateral load tests have been completed on some full-scale offshore piles and the results have shown larger displacements than were predicted by the p-y curve method (Long & Vanneste, 1994). The authors believe that the discrepancy is because the p-y curves fail to account for the nature of the load, its form and the number of load cycles. There is also no allowance made for the difference between installation methods.

So, in summary, not only do the current design methods not apply to piles of the size and rigidity used for wind turbine supports they also do not adequately account for the dynamic nature of the loading.

2.2 Dynamic Behaviour of Wind Turbine Structures

As discussed in the introduction it is important to be able to assess the natural frequency of a wind turbine and its support structure so that damaging resonance can be avoided. One method of finding the natural frequency is to model the turbine as a cantilever fixed at its base, as shown in figure 2.1a. Tempel & Molenaar (2002) conducted such an analysis, they proposed that the fundamental frequency is given by:

$$f_n = \sqrt{\frac{3.04EI}{(M+0.227mL)4\pi^2L^3}} \tag{2.1}$$

Although this equation is convenient because of its simplicity it is arguably an over-simplification of the real situation. Clearly there is little account for the pile-soil interaction, equation 2.1 would give the same results for dense and loose soil conditions.

Adhikari & Bhattacharya (2012) attempted to include the pile-soil interaction by analysing a more complicated model, shown in figure 2.1b. Their model included both a lateral and rotational spring at the base of the turbine to more accurately describe the base fixity conditions. By solving the resulting differential equations the authors were able to formulate dimensionless design charts that would allow designers to quickly estimate the natural frequency of their structures. The difficulty arises in deciding on values to use for the stiffnesses which are dependent on properties of the foundation and soil conditions.

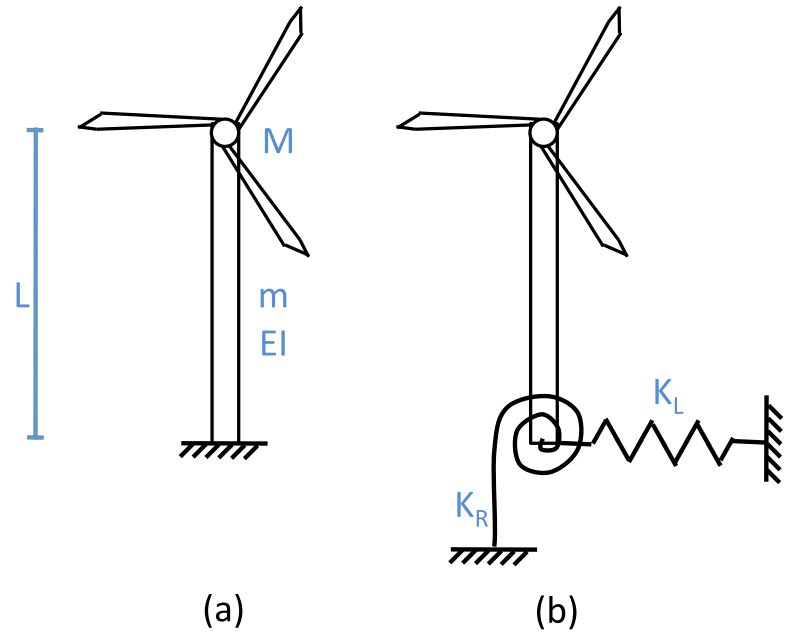

Figure 2.1: Examples of models used for estimating the natural frequency of wind turbine structures (a) Tempel and Molenaar (2002) (b) Adhikari and Bhattacharya (2010).

Some research has aimed to create finite element models of the monopile-soil system; these models can then calculate the displacements and rotations under different load conditions. However soil stress-strain behaviour is non-linear and the numerical models depend on having an accurate constitutive model that can account for the affect that the cyclic loading has on the soil properties. Achmus *et al (2009)* introduce the degradation stiffness model that combines finite element techniques with the results of drained cyclic triaxial tests. Figure 2.2 shows some of the results from the study. The plots show the variation in lateral displacement with depth from the seabed and number of load cycles for two different embedment lengths. The increase in displacement with number of load cycles is clear, as is the reduction in displacements caused by the increase in embedment length. The figure also shows the toe kick that occurs where the pile rotates about a point near, but not at, its base. The researchers found that the model agreed closely with some scaled tests they had completed and they plan to calibrate the model against some full-scale tests in the future.

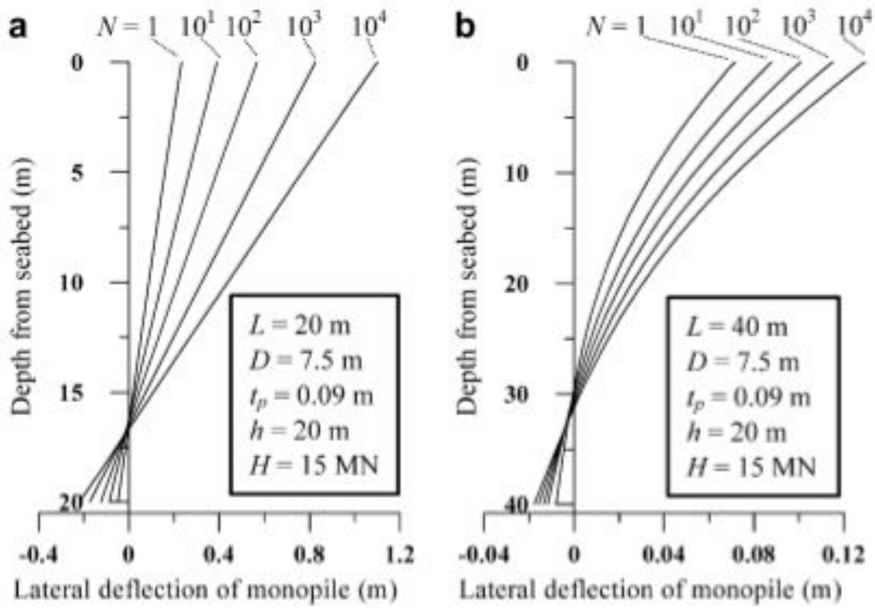

Figure 2.2: Lateral Deflection of Piles According to the Degradation Stiffness Model (Achmus, Kuo, & Abdel-Rahman, 2009).

2.3 Shear Stiffness of Soils in Dynamic Loading Situations

It has been mentioned in previous sections that the dynamic response of the turbine-foundation-soil system is dependent on the stiffness of the soil. The shear stiffness of a soil depends on the magnitude of the strain it is experiencing. At very small strains ($\gamma \approx 10^{-6}$) stress-strain behaviour is approximately linear and controlled by the initial shear modulus, 'G_{max}'. Many empirical formulations for estimating initial shear modulus have been proposed over the years, including equation 2.2 for sandy soils (Hardin & Drenvich, 1972b).

$$G_{\max} = 100\frac{(3-e)^2}{1+e}(p')^{0.5} \tag{2.2}$$

Equation 2.2 shows that the initial shear modulus is dependent on the void ratio, which is representative of soil density, and the mean effective stress. This formulation and other related empiricisms are based on experimental evidence, usually involving the analysis of shear wave velocities, it is known from the theory of wave propagation that shear wave velocity is given by equation 2.3 (Santos & Gomes Correia, 2000).

$$v_s = \sqrt{\frac{G_{\max}}{\rho_{sand}}} \tag{2.3}$$

For medium strains ($\gamma \approx 10^{-6}$ - 10^{-2}) the stress-strain behaviour of soil is distinctly non-linear. These strain levels are typical of many geotechnical applications including wind turbine foundations. This non-linearity makes design much more complicated. This degradation of shear stiffness with increasing strain has been the subject of extensive research. For example Oztoprak & Bolton (2013) used a database of laboratory test data on high quality soil samples to propose a modified hyperbolic stress-strain relationship. The degradation in shear modulus is clear from their curve fit, shown in figure 2.3.

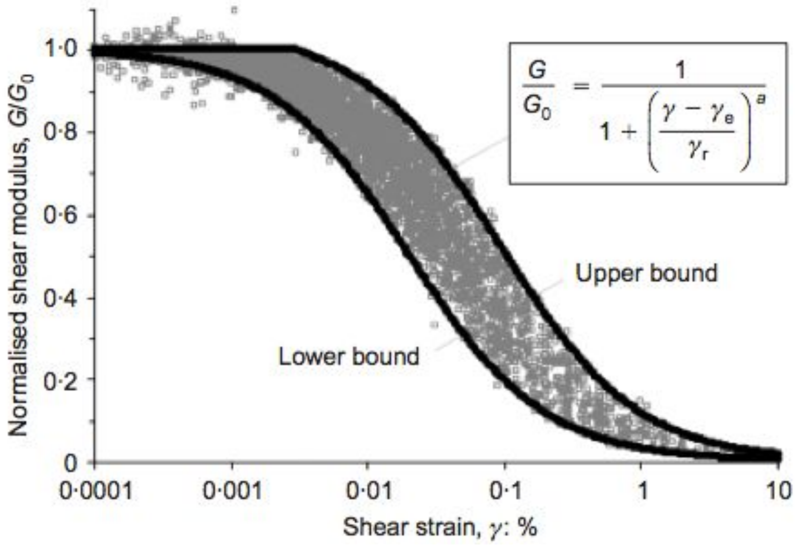

Figure 2.3: Curve fit to laboratory test data showing degradation in shear stiffness with increasing strains (Oztoprak & Bolton, 2013).

It has also been touched on that this shear stiffness can be influenced by the number of load cycles. These behaviours under cyclic loading are not well accounted for in current design methods. For example the current methods always predict that under cyclic loading in sands there will be degradation of foundation stiffness. This is accounted for by degrading the p-y curves. However laboratory testing at 1-g of scaled model monopiles in dry sand have found that cyclic loading always acts to increase the stiffness of the system (LeBlanc, Houlsby, & Byrne, 2010).

2.4 Conclusions

This review of current literature has discussed some of the theories that are behind the current guidelines in the design of offshore wind turbine support structures. It has also noted research that has questioned the validity of these currently accepted methods. In summary; the current methods are based on research for the oil and gas industries that has then been extrapolated to apply to the larger monopiles required for turbine support structures. As well as being used outside of the parameters of this initial research the current methodologies to not adequately account for the nature of the dynamic loading that is applied to wind turbine support structures.

Research has been completed to try and improve the validity of the code methodologies. Mainly this research has been concerned with accumulated rotations and displacements and the influence of the number of load cycles. This project aims to continue the theme of this research but to concentrate more on the dynamic properties of the system. Including how the soil and nature of the loading affects the dynamic response of the system so resonance and vibrations can be more appropriately considered in monopile foundation design.

3.0 Experimental Methods

The experiment was designed as a scaled down version of the full size turbine-monopile-soil system. All experimental work was completed at normal 1-g acceleration levels. All of the experimental work undertaken for this project was completed in the laboratory at the Schofield Centre, University of Cambridge.

3.1 Model Pile

All experimental work used a small-scale hollow aluminium model monopile with an open base. Key properties are summarised in table 3.1. To record the dynamic response of the monopile itself the pile was instrumented with micro-electro-mechanical (MEM) accelerometers. Three 1.7-g accelerometers were affixed with superglue down the length of monopile. There was also a 35-g accelerometer located at the top of monopile if the accelerations here became too large for the smaller accelerometers range. Figure 3.1 shows the model monopile with attached top-plate and instrumentation.

Length, L	450 mm
Outer diameter, D	76 mm
Wall thickness, t	1.7 mm
Second moment of area, I_{xx}	2.74×10^5 mm^4
Young's modulus, E	70 GPa
Mass of monopile	0.475kg
Mass of top-plate	0.270kg
Mass of actuator	0.375kg

Table 3.1: Key properties of the model monopile.

As the MEM accelerometers used were only capable of recording accelerations along one axis it was important that they were all aligned in the direction that the impulse and harmonic loading was applied. Care was also taken to fix associated wiring securely so there were no issues with snagging or breaking during pile installation.

Figure 3.1: Instrumented model monopile.

3.2 Experimental Model Setup

Most of the experiments involved installing the model monopile into an 850 mm diameter tub filled with dry Hostun sand. The model setup is shown schematically in figure 3.2. As well as the instrumentation attached to the monopile accelerometers were placed on a radial line out from the monopile at distances of 0.5D, 1D, 1.5D and 2D; where D is the pile diameter.

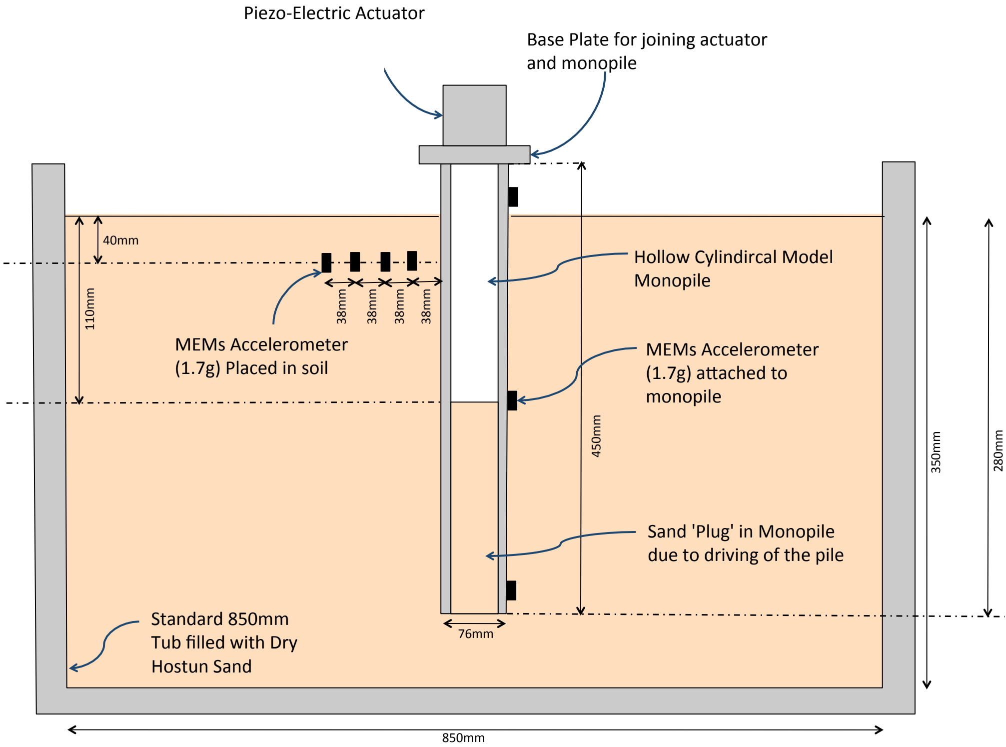

Figure 3.2: Schematic of model setup.

The pile was driven after the first 190 mm of sand had been poured; this created a soil plug within the monopile that is typical in a real installation. It was chosen not to drive the pile when all the sand had been poured as this meant it was easier to make sure the pile was driven vertically. There were also concerns about breaking the attached accelerometers during driving in the denser models. After sand pouring was complete the pile had an embedded length 280 mm and the load was applied 170 mm above the surface of the sand. Figure 3.3 shows a completed model ready for testing.

Figure 3.3: Completed experimental model prior to testing.

3.3 Preparation of Soil

All models were made with dry Hostun sand that was readily available in the lab. The properties of the sand used are summarised in table 3.2. Dry sand was used as it made model preparation quicker and easier and it can be argued that tests are likely to be fully drained so dry sand is appropriate (LeBlanc, Houlsby, & Byrne, 2010). Sand was chosen over clay due to project time constraints, it was decided that more testing could be completed in the same time frame if the soil used was dry sand. Also the soil at shallow depths offshore of the United Kingdom is often comprised of sand deposits (Byrne & Houlsby, 2003)).

Minimum Voids Ratio, e_{min}	0.555
Maximum Voids Ratio, e_{max}	1.067
Specific Gravity, G_s	2.65
Poisson's Ratio, v	0.25

Table 3.2: Properties of Hostun sand.

The sand was poured into the tub from a hopper which allowed the flow rate and drop height of the pour to be controlled. Calibration pours were used to determine the flow rate and drop height required to pour sand at the required relative densities. The loose sand models required a fast flow rate and low drop height. For the dense pours it was necessary to attach a sieve to the hopper to reduce and spread the flow. Also care was taken to maintain the amount of sand in the hopper as this affected the flow rate.

Sand was poured in layers to facilitate the driving of the model pile and installation of the soil instrumentation. All sand pouring was conducted with adequate ventilation.

3.4 Instrumentation

As previously discussed MEM accelerometers were used to measure the response of the model to the loading. Total instrumentation included three 1.7-g accelerometers on the monopile itself and four 1.7-g accelerometers in the soil to give an insight to the transmission of the vibrations through the soil. The MEM accelerometers are small and light so should have minimal effect on the results. They are also relatively inexpensive.

However it was decided that the accelerometers would be too small to truly record the accelerations within the soil as the sand may simply move around them. The accelerometers that were installed in the sand were glued to a 2.5 cm square of flexible plastic, see figure 3.4, this acted to increase the surface area so they were more likely to capture the true response of the soil.

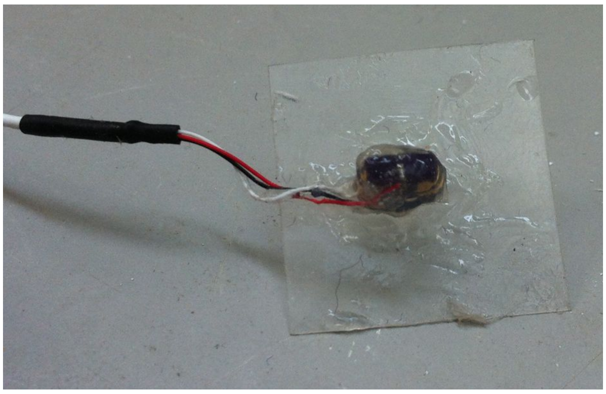

Figure 3.4: MEM accelerometer with plastic backing for use within the sand.

The 1.7-g accelerometers require a 5 Volt power supply and should give an output of 2.5 Volts when there is no acceleration. The output of the accelerometer is meant to change according to the acceleration, with a change of 1 Volt corresponding to a change in acceleration of 1 g with a sensitivity of 0.001 V. In reality there is some variation between the individual accelerometers. All accelerometers were calibrated by subjecting the accelerometer to an acceleration of 1g and -1g and using the difference in the recorded outputs to calculate the Volt-acceleration relationship for each device. The DC component of each output was removed in post-analysis by averaging the initial output of each sample before any loading was applied. Also the data was filtered to remove any high frequency noise from the signals. Filtering was completed using MATLAB's *Butter* function and applied using the *filtfilt* function to minimise any phase distortion due to the filtering process.

All of the accelerometers were connected to a computer and power supply via a junction box. All of the data logging was completed using the DasyLAB 9.0 software. A sampling rate of 40kHz was used. Sampling rates needed to be high because of the small distances between the MEMS in the soil and the high speeds which the shear waves would travel at. However there was an upper limit on the sampling rate due to the number of accelerometers used and the capacity of the data-logging hardware.

3.5 Impulse Testing

The simplest tests conducted were impulse tests; these involved applying an impulse load to the monopile by tapping the top with a spanner. These tests were conducted with the top-plate and actuator attached so that the models were consistent between impulse and harmonic tests. The additional top-mass would have an effect on the system properties.

Multiple impulses were applied for each model that was poured. During these tests the response was recorded by the accelerometers on the pile itself and those in the sand.

As well as conducting impulses on the model monopile embedded in the sand impulse tests were conducted with the base of pile clamped to a rigid frame to prevent rotation. Such that the monopile was acting like a fixed base cantilever. In this case only the accelerometers on the pile itself were useful.

3.6 Harmonic Testing

One-directional cyclic loading was applied at the top of the model monopile using a piezoelectric actuator. This was designed to represent the dynamic loading that a real wind turbine monopile experiences. For each model poured the monopile was loaded at a range of different forcing frequencies. During harmonic tests data was sampled from the accelerometer at the top of the monopile and the four within the sand.

3.6.1 Piezoelectric Actuator

The piezoelectric actuator is attached to the top of the monopile via the top-plate; the actuator is shown in figure 3.5. A signal generator was used to provide a sinusoidal input. The frequency of this input could be adjusted to the desired values. The input signal was amplified with a dedicated amplifier before being passed to the actuator. To remain safely within the operating limits of the amplifier and actuator the input signal had to be maintained at a DC-offset of 3.25 Volts and a peak-to-peak voltage of 5 Volts.

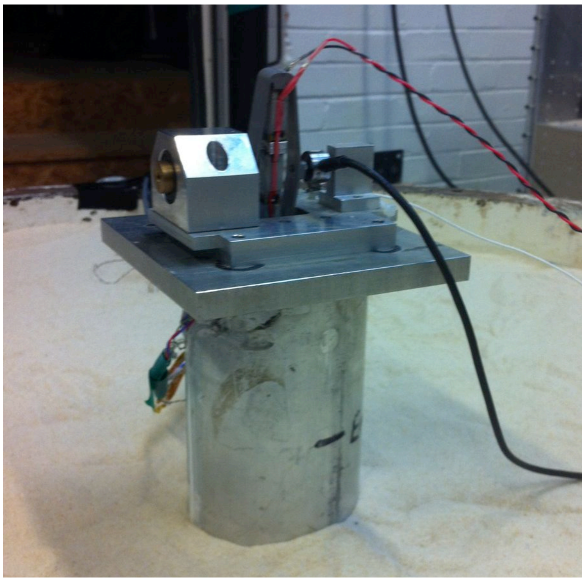

Figure 3.5: The piezoelectric actuator attached to the embedded monopile.

3.7 Model with Additional Top Mass

Further testing was conducted with extra mass attached to the top of the model monopile. The aim was to increase the mass of the structure without altering the stiffness; this would reduce the natural frequency of the structure as:

$$f_n = \frac{1}{2\pi}\sqrt{\frac{K_{eq}}{M_{eq}}} \tag{3.1}$$

Both impulse and harmonic testing was conducted on this altered monopile in a loose sand model. Also fixed base impulse tests were conducted. In these tests an extra 1.27 kg was added to the top of the pile.

4.0 Dynamic Response of the Model Monopile

4.1 Establishing the Natural Frequency of the Experimental Model

4.1.1 Analysis of Impulse Tests

The impulse response as recorded by the 1.7-g accelerometer near the top of the model monopile is used to determine the structures fundamental frequency. The sample data is imported into MATLAB and then the sample is windowed to isolate the relevant transient portion, an example is shown in figure 4.1a. The Fourier transform of the impulse response is computed using MATLAB's fast Fourier transform function, *fft*(signal). The absolute values of the Fourier transform are computed to remove the complex components and then plotted. A peak on this plot will correspond to a natural frequency of the system, an example is shown in figure 4.1b which is for a model poured at a loose relative density. The plot shows a resonant frequency of approximately 104 Hz.

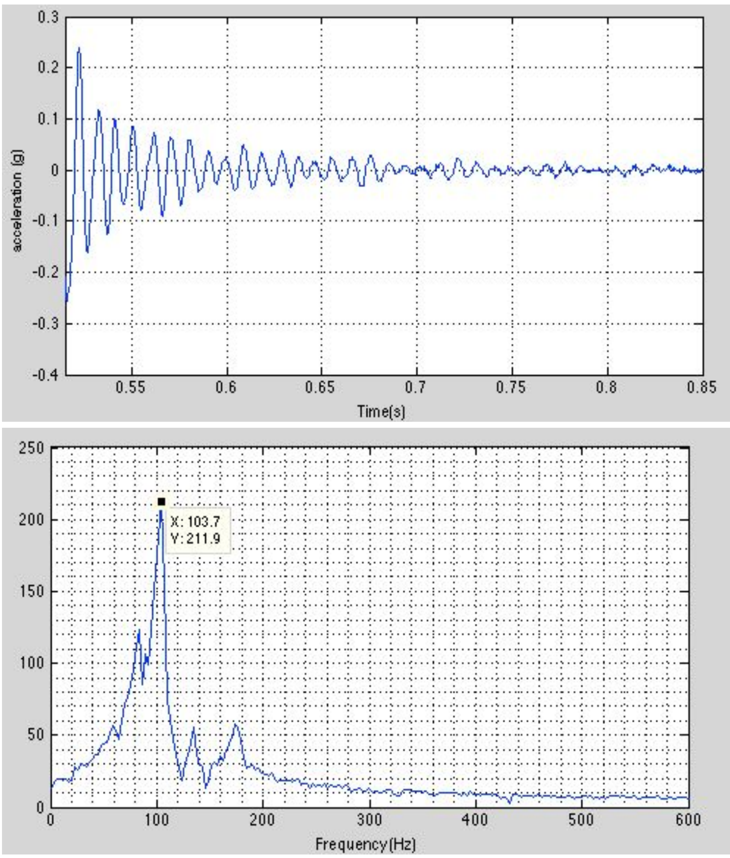

Figure 4.1: For an impulse test on a loose sand model: (a) Windowed impulse Response in time domain (b) Fast Fourier transform of (a)

Signals were windowed as appropriately as possible. Longer samples would give better frequency resolution, however it is the transient part of the response that must be analysed. There would be no point in analysing the noisy portion of the signal when the response had died down or the initial part of the impulse which is noisy due to the method of applying the impulse.

4.1.2 Comparison of Experimental Results

The above analysis was carried out on models poured at different relative densities. Table 4.1 summarises the calculated fundamental frequency for eight impulse tests on a model poured densely with a relative density of 0.75. Clearly all tests were in reasonable agreement with an average calculated natural frequency of 137 Hz.

Test No.	Peak Frequency (Hz)
1	138
2	137
3	137
4	137
5	137
6	137
7	136
8	135
Average:	**137**

Table 4.1: Summary of results of natural frequency analysis of impulse tests on a dense model.

Figure 4.2 below shows a comparison of the Fourier transforms of two impulse responses, one on a dense model and one on a loose model. The main peaks, corresponding to the first natural frequency, are clear and so is the shift in frequency at which the main peak occurs. As expected the loose model has a lower natural frequency, due to the lower soil stiffness.

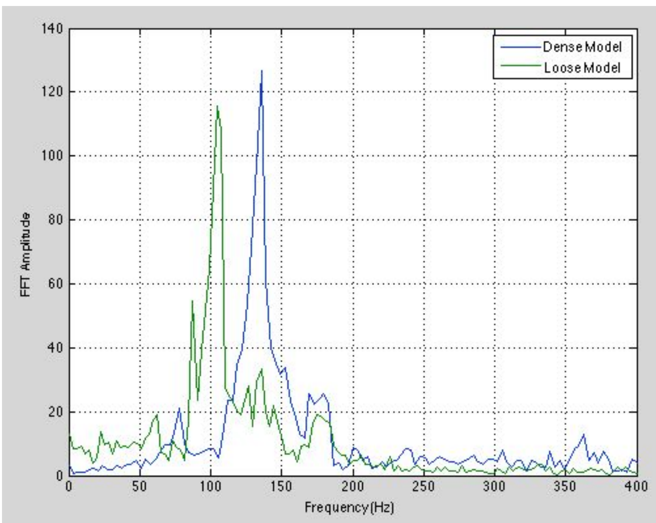

Figure 4.2: Fourier transforms of two impulse responses one from a loose model and one from a dense model.

The average natural frequencies calculated from multiple impulse tests for other models are summarised in figure 4.3. The figure clearly shows the increase in natural frequency with increasing relative density as expected due to the associated increase in soil stiffness. The relationship initially appears approximately linear.

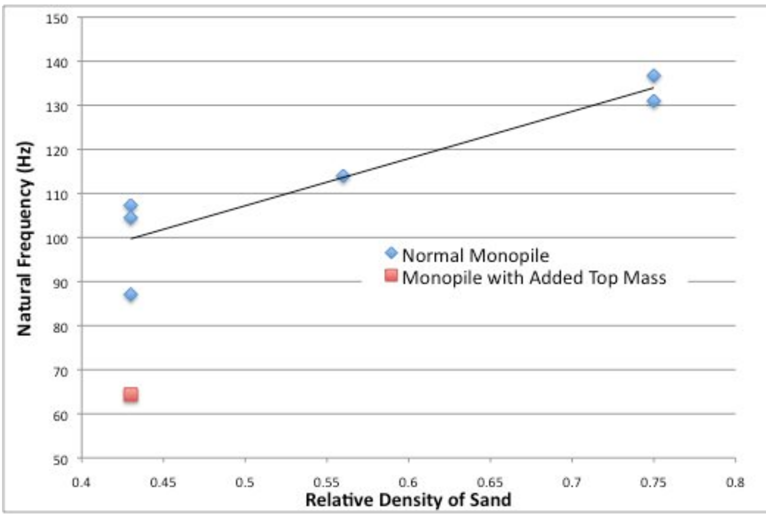

Figure 4.3: Summary of natural frequencies calculated for models of varying relative density.

For the loose and dense models that have multiple data points there is apparent densification of the models. In both cases the longer the model was left after pouring the higher the natural frequency became implying a densification of the sand. This densification is most likely due to the harmonic loading applied to the models between rounds of impulse testing and also some tendency for the sand to settle more densely over time. This means that the relationship may not be as linear as implied by the shown trend line.

Calculating relative density from the mass of sand poured and the measured final volume was quite inaccurate given the setup and large volumes involved. An in-situ method would be better but this would interfere with the experiment, also any readings may be influenced by any local variations in relative density.

4.1.3 Monopile with Added Top Mass

Also shown on figure 4.2 is the result for the monopile in a loose model with extra mass added to the top. As expected, from equation 3.1, the increased mass has caused a significant reduction in the natural frequency from around 105 Hz to 65 Hz. This shift is shown in figure 4.4 which shows the Fourier transforms of two impulse tests performed in the same loose sand model, one with added mass and one without.

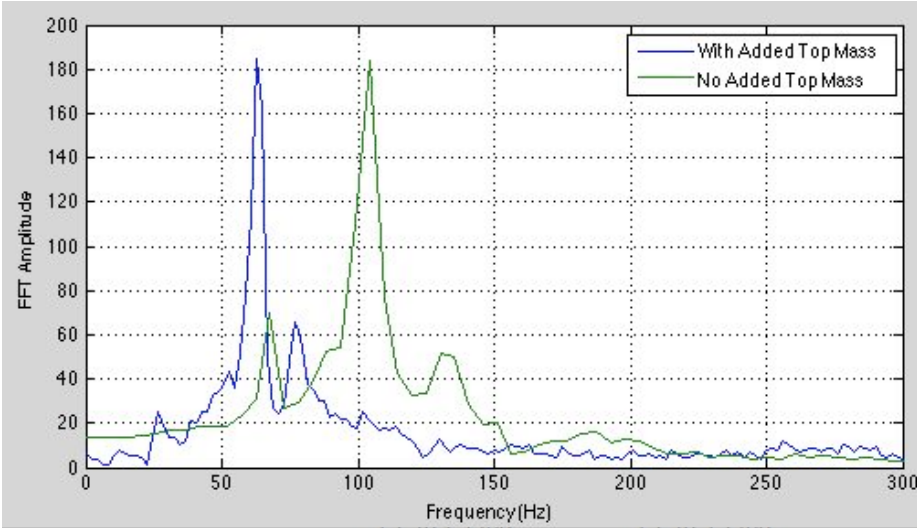

Figure 4.4: The Fourier transform of the impulse response both with and without added top mass in a loose sand model.

4.1.4 Results from Fixed Base Tests

As well as finding the natural frequency of the monopile system in the tubs of soil impulse testing was also conducted on the model pile with the base clamped to a rigid frame so it was acting like a rigid cantilever. Tests were performed both with and without added mass. Figure 4.5 shows a comparison of the Fourier transform of two impulse responses, both with and without the added top mass.

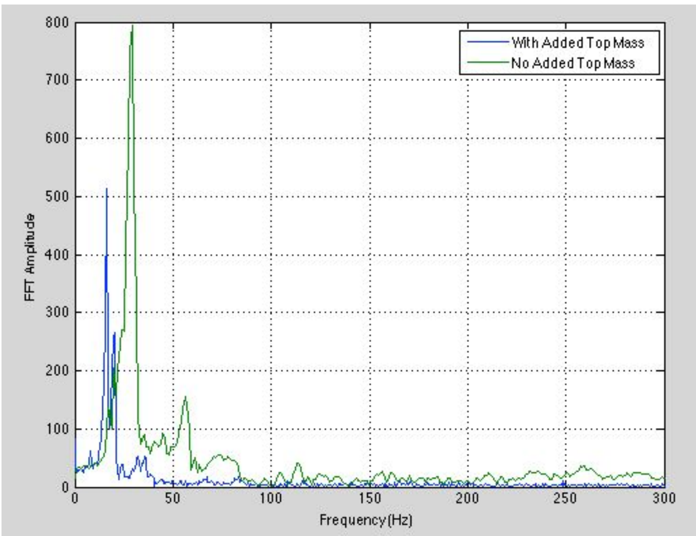

Figure 4.5: The Fourier transform of the impulse response both with and without added top mass with the base rigidly clamped.

The figure highlights the expected reduction in natural frequency that occurs when the extra mass is added at the top of the monopile. The figure shows a drop in natural frequency from 27 Hz to 16 Hz. These frequencies are much lower than the natural frequencies of the monopile when it is embedded in the sand. This is because the sand increases the stiffness of the system a lot; it effectively shortens the effective length of the monopile. Closer natural frequencies may have been obtained if the monopile was clamped at the same level as the sand surface.

The figure shows much cleaner peaks than in the embedded cases. This is probably a benefit of the longer sample used to calculate the Fourier transform which was possible due to the decreased damping, it also reflects on the reduced complexity of the clamped system. Furthermore the added mass case shows a smaller peak than the normal case, this would be explained because roughly the same force was applied in both cases but the extra mass would have meant smaller accelerations. Although in both cases the amplitude is approximately four times higher than the embedded cases, which is because of the reduced stiffness of the system meaning greater accelerations are generated for a given force. Another thing to note is that the impulse response for the fixed base cases lasts much longer than the in soil case, the difference is around one order of magnitude. This is to be expected as the soil will act to increase the damping in the system.

4.2 Damping in the System

The overall damping in the system can be roughly estimated from the impulse response using the logarithmic decrement. The damping ratio, 'ζ', can be calculated from the equation for logarithmic decrement (4.1).

$$\ln\left(\frac{y_1}{y_2}\right) = \frac{2\pi\zeta}{\sqrt{1-\zeta^2}} \tag{4.1}$$

Where y_1 and y_2 are the heights of two successive maxima.

Analysis of the fixed base tests suggests a damping ratio of around 6%. As expected the embedded models exhibit increased damping. Typically the loose models had a higher amount of damping with a damping ratio of approximately 26%. This was compared to a typical dense model which gave a damping ratio of approximately 17%. Once again this highlights how the properties of the soil have a significant impact on the dynamic properties of the monopile.

4.3 Response to Harmonic Loading

4.3.1 Variation of Pile Head Accelerations with Forcing Frequency

As described in section 3.6 the dynamic loading was applied to the model monopile with a piezoelectric actuator. The frequencies applied were generally in the range 60 Hz – 170 Hz, at lower frequencies the actuator didn't give a smooth sinusoidal loading and above 170 Hz the force applied by the actuator meant that accelerations at the top of the pile began to exceed the range of the accelerometer in that location. Figure 4.6 shows how the acceleration at the top of the pile varies as the forcing frequency of the load is increased.

Plotted on the figure are the results from a loose model and a dense model, for each model two rounds of identical harmonic testing were completed, the A and B tests. The results of both A and B tests are shown to highlight the agreement between the results. This shows the experiment is repeatable and consistent. In both cases the upward trend is clear, this is because at higher frequencies the actuator applies a higher force because the actuator must make the same displacements in a shorter time period. Unfortunately problems with the load cell meant that the results could not be normalised with respect to input force.

However in both cases when driven at frequencies close to the natural frequencies, as calculated in section 4.1, the responses have smaller magnitudes than the general upward trend would suggest. This is at odds with the normal idea of resonance where a structure shakes itself to pieces. One possible explanation is that at these frequencies the surrounding sand at its respective densities is dissipating more of the energy put into the system by the actuator away from the pile so that the vibrations of the actual pile are damped more effectively. However it may also be the case that at these frequencies the structure is trying to vibrate in a different mode shape than the one the actuator is trying to force, this could lead to a reduced overall response.

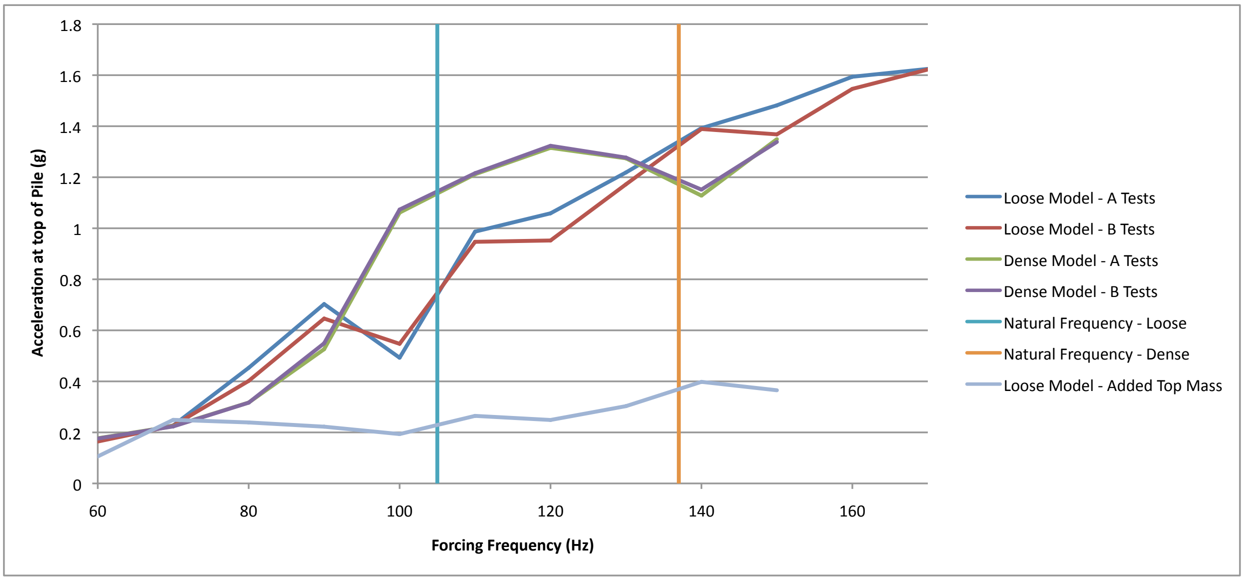

Figure 4.6: Variation of pile head acceleration with increasing forcing frequency, for both loose and dense models.

Also shown on the figure is the response recorded for the monopile with added top mass. The response still shows the general upward trend but the magnitude of the response is lower than the normal tests. This is because the increased mass of the monopile but the same piezoelectric actuator translates to smaller accelerations. There is no distinguishable trough on the plot but the resonant frequency for this model was found to be at 64 Hz. The initial rise of the response is steep from around this value.

5.0 Ground Borne Vibrations

5.1 Calculation of Shear Wave Velocity

By analysing the impulse response recorded by the accelerometers in the sand it is possible to calculate the velocity of the shear waves caused by the loading. In the first few experimental setups the soil accelerometers were placed on two separate levels, two near the surface and two on a deeper level. The main problem with this setup was that the accelerometers near the surface were too shallow and the very low confining stress meant the accelerometers were likely to shift out of their position and generate spurious results. Furthermore the deep instruments were only experiencing very small accelerations and so post-analysis did not yield very interesting data.

It was decided to reconfigure the layout as detailed in section 3.2 with all the accelerometers on the same level and at a slightly deeper depth. It was thought that this would provide a more detailed picture of the wave transmission, provide redundancy against instrument failure and the higher confining stress should stop the accelerometers from moving out of position.

5.1.1 Method of Analysis

As the distance between the accelerometers is fixed and known the speed can be calculated by measuring the difference in arrival times between the different instruments. Initially the arrival times were determined manually by manipulating the four different signals to identify the arrival times of the first peaks. Figure 5.1 shows part of the time traces from a test in loose sand. The figure highlights how small the time lag is.

The manual method took quite a long time and was not suitable for the large number of samples that needed analysing. A more suitable method was employed which used MATLAB's *xcorr()* function. This function takes two samples and computes the cross-correlation. The cross-correlation is a mathematical comparison of the two signals and outputs their similarity as a function of the time-shift between the two. In this case the two signals should have very similar form and so the time-shift which gives the maximum value of cross-correlation will represent the difference in arrival times at the two instruments sampled. The output of the function is given as the lag in number of samples but this is simply converted to a time by considering the sampling frequency, 40 kHz corresponds to a period of 0.000025 seconds per sample.

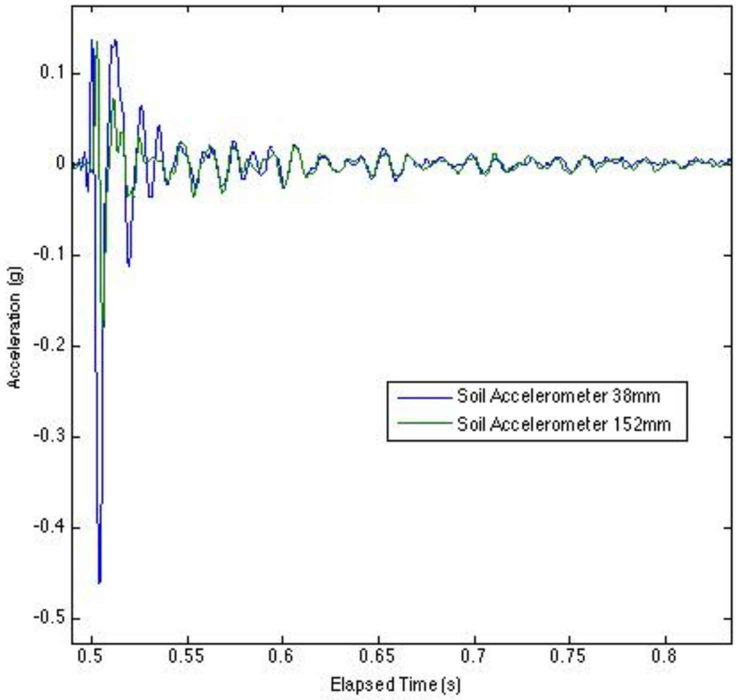

Figure 5.1: Example time trace from the near and far soil accelerometers in a loose sand impulse test.

The cross-correlation method was found to agree closely with the analysis that had been conducted manually and so was used for future analyses. The function was easily incorporated into a script so that the difference in arrival times between any pair of the four accelerometers was calculated with ease.

5.1.2 Experimental Results

This analysis was completed for a number of different density models, table 5.1 summarises the results for impulses applied to a loose sand model with a calculated relative density of 43%. The results are shown for the cross-correlation between the closest (38 mm) and furthest (152 mm) accelerometers in the soil. The result for impulse number six was not included as there were problems with the data sampling that lead to a calculated wave speed of 43 ms^{-1}. Apart from this one anomaly results are in good agreement and suggest an average wave speed of 87 ms^{-1}. The results are also very consistent considering that all results are no more than three samples away from the average.

Impulse Number	Difference in arrival time (in samples)	Wave Speed (ms^{-1})
1	53	86
2	52	88
3	55	83
4	55	83
5	52	88
7	51	89
8	50	91
9	55	83
10	51	89
	Average:	87
	Standard Deviation:	3.2

Table 5.1: Shear wave velocity results for a loose sand model.

Figure 5.2 shows some of the other experimental results. Unfortunately not many data points could be included because of problems with instrumentation. Mainly this was due to the low sampling rates that were used in early tests that led to inconsistent and unreliable results.

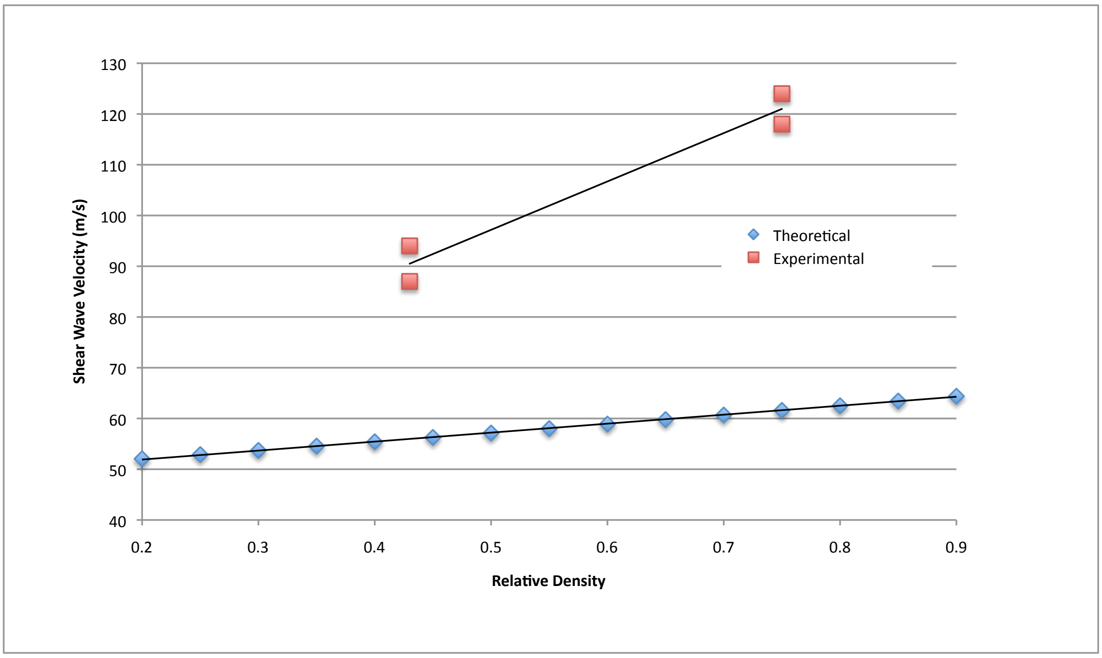

Figure 5.2: Plot of experimental and theoretical variation of shear wave velocity with relative density of sand.

However the expected increase in shear wave velocity with increasing relative density is shown by the experimental results. What is interesting is that for both the loose and dense models shown there are two data points. These pairs represent two sets of impulse tests that were applied to the same model but with the second tests were applied when the model had been left untouched for a few days. The increased shear wave velocity in both cases suggests that the models have undergone some amount of densification. Figure 5.3 shows the shear wave velocities plotted as a function of the calculated natural frequency for each model; see section 4.1.

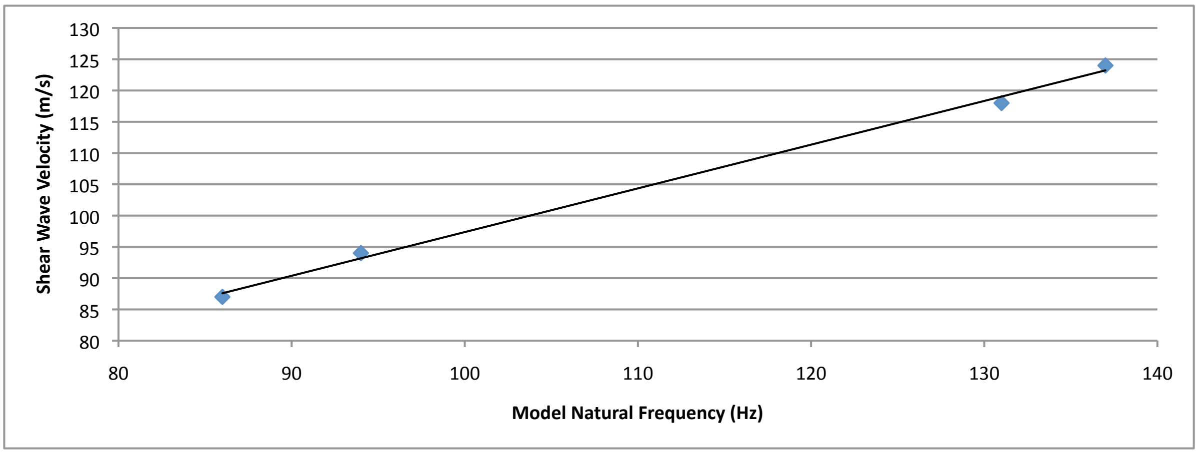

Figure 5.3: Plot showing the relationship between calculated shear wave velocity and calculated natural frequency of the experimental models.

Presented in this fashion the experimental results fall more convincingly onto a line. This is as expected as both the increased natural frequency and the increased velocity are related to increased soil stiffness. This apparent densification of the models is likely to be a result of the harmonic loading applied to models after each round of impulse tests. There may also be some compaction of the sand with time as it is left untouched.

5.1.3 Comparison with Theory

Also shown on figure 5.2 is a line representing the theoretical shear wave velocity. This is calculated based on the empirical calculation for shear modulus given by equation 5.1 from Hardin and Drenvich (1972).

$$G_{\max} = 100\frac{(3-e)^2}{1+e}(p')^{0.5} \qquad (5.1)$$

where the voids ratio, e, is calculated from the relative density according to (5.2).

$$I_D = \frac{e_{\max} - e}{e_{\max} - e_{\min}} \qquad (5.2)$$

Confining stress is estimated by combining the following expressions and assumptions, assuming a Poisson's ratio of 0.25 for sand in drained conditions, z =0.04m, γ_{water}=10kN/m^3.

$$p' = \frac{\sigma'_v + 2\sigma'_h}{3} \;\; ; \; \sigma'_h = K_o\sigma'_v \;\; ; \;\; K_o = \frac{\nu}{1-\nu} \;\; ; \;\; \sigma'_v = \frac{G_s\gamma_{water}z}{1+e} \qquad (5.3)$$

Calculation of the theoretical shear wave velocity is then simply according to equation 5.4.

$$v_s = \sqrt{\frac{G_{\max}}{\rho_{sand}}} \tag{5.4}$$

The theoretical line shows the expected increase in shear velocity with relative density however the increase is at a slower rate and the velocities are much lower than those calculated from the experimental data. This discrepancy is probably due to the empirical formulation not being appropriate for confining stresses as low as considered in these tests. The low confining stresses are also likely to lessen the validity of some of the expressions in 5.3. There are also issues with the accuracy in calculating the relative density of the models accurately due to the large volumes of sand involved.

5.1.4 Monopile with Added Top Mass

Impulse tests were performed in a loose density model with the monopile in its normal configuration and then with an added 1.27kg of mass added to the top of the monopile. Unfortunately issues with instrumentation meant that the only reliable indication of shear wave velocity could be calculated from the nearest two instruments, so a separation of only 38 mm. With no added mass the average velocity was calculated as 64 m/s and with added mass this increased to 100 m/s.

This result is interesting because the velocity of the shear waves should be governed by the stiffness of the soil and changing the mass of the pile shouldn’t affect this soil parameter. The increase also seems too large to be explained by densification of the sand due to the loading as previously discussed. Further testing is required.

5.1.5 Model Limitations

With the manual pouring methods employed for this project it is hard to guarantee that the sand relative density is uniform throughout, it is also very hard to measure the relative density after the sand has been poured without disturbing the model. Calculation of relative density relied on accurately recording the amount of sand poured into the model as well as calculating the volume accurately. Clearly a better way of measuring the relative density of the sand is needed. Perhaps the relative density could be better controlled through the use of an automatic sand pourer. This would, however, increase the time taken to prepare each model.

There were quite a few issues with instrumentation; these were mostly the result of the accelerometers in the sand moving out of position. As the separation of the instruments was small and wave speeds were high, the results of this analysis were very sensitive to the distance between the accelerometers. Accelerometers were arranged in 38 mm intervals, corresponding to half of the pile diameter. Considering the actual accelerometers are 5mm long it is hard to guarantee the exact location accurately. This is why the calculated wave speeds were based on the largest separation between the nearest and furthest instrument. However this had the complication that by the time the shear wave had reached the furthest accelerometer the magnitude of the accelerations are quite small so the effects of noise and filtering become more significant.

The option of locating the soil accelerometers deeper to take advantage of larger confining pressures was dismissed. Although it would reduce the likelihood of the accelerometers moving excessively out of position it would also mean that the magnitude of the accelerations would have been reduced even further as they are further away from the source and so exacerbating issues with the signal processing. One viable option would be to conduct further tests in a geotechnical centrifuge, this would increase the confining stresses to more realistic values without having to bury the accelerometers deeper.

The affect of boundary conditions on the experimental results should also be considered. The boundaries of the tub are clearly not entirely representative of the semi-infinite extent of the soil layers that would be present in the real situation. However in terms of radial distance the small magnitude of the accelerations at the furthest soil instrument (190 mm from the centre of the tub, radius 425 mm) suggest reflection of waves back into the centre of the model from the tub sides is not a significant issue. Perhaps more of an issue is the effect that four accelerometers with 2.5 cm by 2.5 cm plastic backing would have on the propagation of the shear wave.

5.2 Propagation of Shear Waves through Soil Under Harmonic Loading

The first analysis of the propagation of the shear waves through the sand whilst the monopile was cyclically loaded was by simply looking at the steady-state peak magnitudes of the accelerations as recorded by the instruments in the soil. Figure 5.4 summarises the results of this analysis for a loose and a dense model. In the figure the accelerations are made dimensionless by dividing them by the acceleration of the pile head at each frequency, see section 4.2. As expected the magnitude of the accelerations decrease as distance from the monopile increases at almost all forcing frequencies.

In both models there is a clear peak when the forcing frequency is close to the natural frequency of the system, as calculated in section 4.1. Also generally the responses seem bigger in the loose model. The separation of the top and bottom lines are an indication of the damping that occurs between the nearest and furthest of the in-soil accelerometers. There is some variation in damping with frequency. Calculations of the separation show that on average the response at the furthest accelerometer is 55% of the response at the closest accelerometer in the dense case and 48% in the loose case. This suggests less damping in the dense model although there is not much difference. This concurs with the logarithmic decrement analysis of the impulse response.

This analysis ignores the development of the different frequency components as the waves propagate through the soil. This is looked at further in the next section.

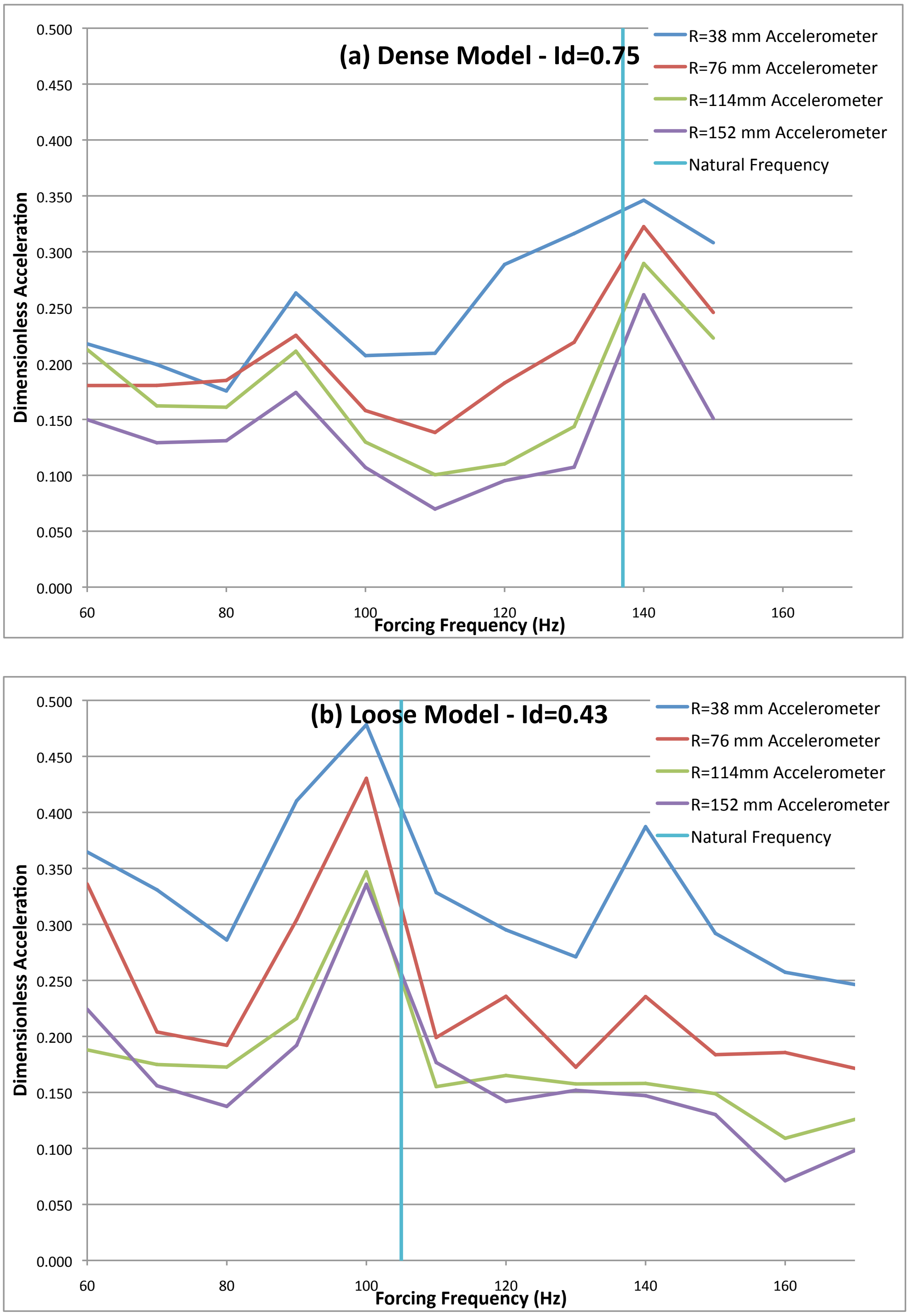

Figure 5.4: Variation of the amplitude of accelerations within the soil as the forcing frequency is varied for (a) Dense model and (b) Loose model.

5.3 Response in the Frequency and Time Domain

So far analyses have been restricted to either the time domain or the frequency domain separately. Wavelet analysis allows the signal to be decomposed into its frequency components whilst still retaining information about the time elapsed by representing the signal on a contour map. 3-D Mesh surfaces can also be made but these did not lend themselves to being reproduced concisely in this report.

This sort of analysis gives insight into how different frequency components occur at different stages of the loading. Figure 5.5 shows ten contour maps, these are the result of a wavelet analysis of an impulse response for both a loose and a dense model. The signal from the accelerometer at the pile head as well as the signals from the four accelerometers in the sand have been processed. The brighter colours indicate a larger power density. The plots for the pile accelerometer both show a high initial peak close to 100 Hz; again for the dense model this peak is at a higher frequency. The magnitude of this peak then decreases with time. In both cases the maps are reasonably clean with the one peak dominating.

The plots corresponding to the accelerometers in the soil are less clean; although in all cases the component at the main natural frequency is present as the dominating peak there are other frequencies that begin to emerge. In the dense model there are noticeable higher frequency components even in the nearest soil accelerometer. Where as in the loose model these higher peaks to not occur noticeably until the third accelerometer.

Figure 5.6 is another ten contour plots. This time the figure shows the wavelet analysis of the harmonic response at a forcing frequency of 90 Hz. The signal was windowed to include the start of the loading and was long enough to contain a significant portion of the steady state response. In all cases the responses start off quite noisy as the actuator is turned on but this part of the response quickly dies down. For both models the accelerometer on the pile has the largest peak at 90 Hz this is to be expected because this is the frequency at which the system is being forced. Also visible are harmonics of this initial peak although these have a much smaller magnitude.

Like the case of the impulse response the plots from the accelerometers in the sand show the other harmonics becoming more significant.

Place holder: Figure 5.5 Wavelet analysis of an impulse response for a loose and dense model

Place holder continued: Figure 5.5 Wavelet analysis of an impulse response for a loose and dense model

Place holder continued: Figure 5.6 Wavelet analysis of a harmonic response for a loose and dense model

Place holder continued: Figure 5.6 continued Wavelet analysis of a harmonic response for a loose and dense model

In the case of the dense model the second harmonic at approximately 180 Hz quickly becomes more significant than the fundamental peak even though it is hardly present in the contour plot from the pile accelerometer. This is similar to the behaviour from the impulse response. Another interesting note is that in figure 5.6 the plot for the 76 mm accelerometer in the dense model there is evidence of the third harmonic, 270 Hz, peaking in pulses.

For the loose model the peak at 90 Hz remains dominant throughout, this is probably because the 90 Hz driving frequency is close to the resonant frequency of the loose model which means that this 90 Hz part of the response continues to increase and so isn't drowned out by the higher harmonics. Figure 5.7 shows the wavelet analysis of the harmonic response measured at the accelerometer 76 mm from the monopile at 110,130 and 150 Hz for the dense model. In the 110 and 150 Hz cases there is a clear peak at the second harmonic, although it is not as dominating this time. However for the 130 Hz case, which is close to the calculated natural frequency of this dense model, the second harmonic peak is not present. This agrees with the behaviour of the loose model at 90 Hz.

In summary, this analysis would suggest that the soil acts to spread the energy from the input force across a range of different harmonic frequencies. However when forced close to the systems natural frequency this effect is lessened due to the resonance.

Place holder for Fig5.7 wave analysis of dense model at different forcing frequencies

6.0 Conclusions

This project aimed to qualitatively assess the dynamic response of monopile foundations in dry sand through the testing of small-scale models at 1-g. The importance of pile-soil interaction was assessed by varying the density of the sand. This project aimed to build on the work in previous years by incorporating instruments into the soil body itself to assess the propagation of the vibrations through the soil. Impulse loading and harmonic loading were applied to the model pile and a variety of analyses at differing levels of sophistication were carried out.

Simple Fourier analysis of the accelerations experienced at the top of the pile was used to determine the natural frequency of the foundation-soil system. It was shown that there was a clear relationship between the density of the sand and the natural frequency of the system. Denser sand pours gave a much stiffer response with a higher natural frequency.

Analysis of arrival times of the impulses at the different accelerometers in the sand allowed the calculation of the shear wave velocity in the model. The calculated values were higher than those predicted by empirical formulations but it was concluded that these empirical formulations are not calibrated for confining stresses as low as experienced in these models. Although the experimental results were as expected in the respect that denser sand generated higher shear wave velocities.

The logarithmic decrement was used as a simple analysis of the damping in the system when subjected to an impulse loading. Results showed that as expected the monopile experienced much greater damping when embedded in the sand. Loose sand resulted in higher damping than dense sand.

Wavelet analysis of the impulse and harmonic responses has shown that the soil seems to spread the energy of any input over a range of harmonics with some higher frequencies dominating the response instead of the driving frequency. This is unlike the turbine itself, which remains predominantly at the frequency of the input. However when harmonic loading close to the systems natural frequency is applied the whole system responds at that frequency with the other harmonics remaining at a small magnitude. This is important for real turbines; it shows that at certain frequencies the whole system will resonate. With the increased magnitude of excitation the stiffness of the soil may change quicker than expected due to the cyclic loading. Furthermore the soils ability to increase the magnitude of higher harmonics is important. The vibrations may occur at a frequency that is damaging to nearby sensitive equipment or be increased to an extent that it is notable and annoying to nearby residents.

The real situation is obviously much more complicated than the models used throughout the course of this project. In the real world a designer has to tackle much more varied site conditions with soil profiles that may vary with depth. There may also be some interaction effects when multiple turbines are placed in close proximity, which is typical of a wind farm. This complexity is why simple models, like those used in this project, are needed. They allow the different variables and responses to be isolated and explained. Although these 1-g models are limited to providing qualitative results they provide useful insights. Hopefully the observations made and the techniques developed through this project will guide more sophisticated analysis in the future. Some suggestions for future experimentation are discussed below.

6.1 Suggested Future Work

It would be beneficial to conduct more testing similar to tests in this project to further corroborate the results. Firstly it would be useful to do further tests in sand of intermediate relative densities to better define the trends that have been outlined by the work completed to date. Then it would be interesting to change some aspects of the model to investigation the importance of other variables. As the importance of the soil density on the pile-soil interaction has already been identified it would be appropriate to see the effect of altering pile properties. The first item to change would be the monopile itself. The model used in this project was quite stiff and rigid and just like the stiffness of the soil has been shown to influence the response the stiffness of the monopile will also. A monopile of similar dimensions but made of a material like PVC would be much more flexible.

It would also be beneficial to change the soil. In this project only dry sand was considered. Perhaps looking at including clay or layers of different densities would make the research applicable to a wider range of real site situations. Other things to investigate at the 1-g level could include the variation of the vibrations with depth or the interaction of multiple monopiles. This project also neglected the effect that the number of load cycles has on the system.

One of the main drawbacks of the experimentation completed during this project was that at 1-g the stresses within the soil are not representative of the real life situation. This alters a number of effects like the stiffness of the soil and the effect that cyclic loading will have on the densification of the soil. It may be pertinent to conduct some of the tests in a geotechnical centrifuge. When geotechnical centrifuges are used the models can replicate real size soil stresses by spinning the models at high accelerations. These centrifuge models are more sophisticated and time consuming than static tests but can provide qualitative results that can be directly applied to full size designs. However static tests still provide a means of getting qualitative results in a quick and cheap manner.

It would also be interesting to conduct full scale testing by instrumenting some existing wind turbines. Full scale testing of a few case studies with accelerometers to monitor ground vibrations would provide useful benchmark studies that could help to focus further scaled testing whether at 1-g or in a geotechnical centrifuge. These full-scale tests could give an idea as to exactly what loads are applied to a wind turbine structure during its working life as well as the behaviour of the vibrations in the surrounding soil. By looking at these case studies the small scale experiments could then be used to predict the response in differing ground conditions.

7.0 References

Achmus, M., Kuo, Y., & Abdel-Rahman, K. (2009). Behaviour of monopile foundations under cyclic lateral loads. *Computers and Geotechnics , 36*, 725-735.

Adhikari, S., & Bhattacharya, S. (2012). Dynamic analysis of wind turbine towers on flexible foundations. *Shock and Vibration , 19*, 37-56.

BERR. (2008). *UK Renewable Energy Strategy Consultation.* London: Department for Business Economy and Regulatory Reform.

Bhattacharya, S., Muir Wood, D., & Lombardi, D. (2011). Similitude relationships for physical modelling of monopile-supported offshore wind turbines. *International Journal of Physical Modelling in Geotechnics , 11* (2), 58-68.

Brødæk, K. T., Møller, M., Sørensen, S. P., & Augustesen, A. H. (2009). *Review of p-y relationships in cohesionless soil.* Technical Report, Aalborg University, Department of Civil Engineering.

Briaud, J. L., Smith, T. D., & Meyer, B. J. (1984). Using pressuremeter curve to design laterally loaded piles. *Proc. of the 15th annual offshore technical conference.* Houston.

Burke, J. (2012). The Dynamic Response of Model Monopiles. *CUED IIB Project 2011/12* .

Byrne, B. W., & Houlsby, G. T. (2003). Foundations for Offshore Wind Turbines. *Philosophical Transactions: Mathematical, Physical and Engineering Sciences , 361* (1813), 2909-2930.

Department of Energy & Climate Change. (2012). *Digest of United Kingdom Energy Statistics 2012.* London.

DNV. (2004). *Offshore Standard: Design of offshore wind turbine structures.* Hellerup, Denmark: Det Norske Veritas.

DONG Energy. (2012). *First foundation launches construction of offshore wind.* Retrieved 2013-15-5 from http://www.dongenergy.com/EN/Media/Newsroom/News/Pages/Firstfoundationlaunchesconstructionofoffshorewindfarm.aspx

European Commission. (2008a). *Proposal for a Directive of the European Parliament and of the Council on the promotion of the use of energy from renewable sources.* European Commission, Brussels.

Hardin, B. O., & Drenvich, V. P. (1972b). Shear modulus and damping in soils: design equations and curves. *Journal of Soil Mechanics and Foundations Division , 98* (7), 667-691.

LeBlanc, C. (2009). *Design of Offshore Wind Turbine Support Structures.* Ph.D Thesis, Aalborg University, Denmark, Department of Civil Engineering.

LeBlanc, C., Houlsby, G. T., & Byrne, B. W. (2010). Response of stiff piles in sand to long-term cyclic lateral loading. *Géotechnique , 60* (2), 79-90.

Liingaard, M. (2006). *Dynamic Behaviour of Suction Caissons.* Ph.D Thesis, Aalborg University, Denmark, Department of Civil Engineering.

Lombardi, D., Bhatacharya, S., & Muir Wood, D. (2013). Dynamic soil-structure interaction of monopile supported wind turbines in cohesive soil. *Soil Dynamics and Earthquake Engineering , 49*, 165-180.

Long, J., & Vanneste, G. (1994). Effects of cyclic lateral loads on piles in sand. *Journal of Geotechnical Engineering , 120* (1), 225-244.

Oztoprak, S., & Bolton, M. D. (2013). Stiffness of sands through a laboratory test database. *Géotechnique , 63* (1), 54-70.

Reese, L. C., & Impe, W. F. (2001). *Single Piles and Pile Groups Under Lateral Loading.* London: Taylor & Francis.

Reese, L., & Matlock, H. (1956). Nondimensional solutions for laterally loaded piles with soil modulus assumed proportional to depth. *8th Conf. on Soil Mechanics and Foundation Engineering. 29.* Austin: University of Texas.

RenewableUK. (2012). *Wind Energy in the UK State of the Industry Report 2012.* London: RenewableUK.

Santos, J. A., & Gomes Correia, A. (2000). Shear modulus of soils under cyclic loading at small to medium strain level. *12th World Conference on Earthquake Engineering.* Auckland, New Zealand.

Tempel, D. P., & Molenaar, D. P. (2002). Wind turbine structural dynamics - A review of the principles for modern power generation, onshore and offshore. *Wind Engineering , 26* (211-220).

UK Government. (2008). *Climate Change Act 2008.* UK Government.

Appendix A: Risk Assessment Retrospective

At the beginning of this project a risk assessment was carried out and handed into the Department Safety Office. As well as this preliminary assessment a Project Approval Document (PAD) was completed and signed by staff at the Schofield Centre before any experimental work in the lab began. Between these two documents most risks associated with this project work were identified and managed. The main items of concern were:

- Inhalation of dust and sand particles during the pouring of the models.
- Injuries associated with manual handling of 25 kg bags of Hostun sand.
- Risks associated with working in a lab environment, such as trip hazards.

These risks were mitigated by adhering to general rules for working in the lab at the Schofield centre as identified in the initial lab induction and the document “10 safety rules for working at the Schofield Centre”. These included wearing a ventilated safety visor whilst pouring sand as well as using a portable ‘DustHog’ extractor unit. Also lab work was only conducted during working hours whilst lab technicians were present.

In hindsight two simple improvements could have made the risk assessment more comprehensive:

- More effort should have been made to update the risk assessment as the project progressed and experimental methods evolved, it is quite hard to identify all risks straight from the outset. Also risk assessment shouldn’t be viewed as a one-time requirement.

- In the original risk assessment the amount of computer use associated with the project was not fully considered. Time spent analysing data and writing up was significant and so the implications of this prolonged computer use should be considered, just as it would be in an office work environment.

It should be noted that there were no injuries or dangerous occurrences throughout the duration of this project.